AIAA JOURNAL
Vol. 33, No. 3, March 1995

Acoustic Study of B Helical Mode for Choked Axisymmetric Nozzle

Michael K. Ponton* and John M. Seiner†
NASA Langley Research Center, Hampton, Virginia 23681

An acoustic near-field study was performed for an axisymmetric conical convergent nozzle operating at a pressure ratio corresponding to a fully expanded Mach number of 1.3. The acoustic measurements were performed in the nozzle exit plane using multiple sensors arranged around the periphery of the nozzle. The acquired data were simultaneously digitized. The acoustic spatial characteristics, describing the large-scale structure associated with the preferred shear layer instability mode, were determined for the dominant B screech mode. The nozzle was fitted with a lip thickening device to determine the effect of this geometric variable on the spatial structure of the jet. For the thin-lipped configuration, the flapping structure of the B screech mode was found to precess in a time-dependent manner about the jet axis. Increasing of the nozzle exit lip thickness altered the spatial characteristics of this mode from a flapping to a time-dependent flapping or spinning. Using the autobicoherence spectrum, frequency dependencies were found to exist in the acoustic data of the thick-lipped configuration. These dependencies may be related to the nonlinearity of the jet and/or the time-dependent nature of the B mode spatial structure.

Introduction

THE classical approach in understanding a turbulent flow consists of modeling the flow as the summation of random turbulent instabilities and an average or mean flow.[1,2] These random fluctuations may grow temporally or spatially.[3] Recent experimental work[4,5] suggests that, in addition to the random fluctuations and the mean flow, free shear flows may contain organized wavelike structures which may be deterministic. These organized preferred instability modes are referred to as large-scale structures because they exhibit spatial magnitudes of orders near that of the mean flow. They are also referred to as instability waves because of their local wavelike characteristics.[6]

The study of large-scale structures[7,8] and their relationship to noise generation[9,10] has special significance if one is attempting to understand fluid dynamic properties based on acoustic measurements. Using acoustic and optical measurements, Powell[11] surmised that plume resonance (which causes an intense narrow-band acoustic emission referred to as jet screech) was caused by a feedback process. In his model, an embryo disturbance is shed at the nozzle exit and is amplified as it convects downstream. Interaction of the shock cells with this disturbance causes them to oscillate and produce sound. This sound then propagates upstream outside of the plume and creates new embryonic disturbances at the orifice, which closes the feedback loop. The relationship of screech to large-scale structures using linear spatial stability theory was first introduced by Tam et al.[10]

Full-scale studies[12] have shown significant acoustic energy associated with this noise mechanism causing, in some cases, sonic fatigue of airborne structures.[13] Because no known aircraft utilizes nozzles that produce shock-free flows, accounting for the presence of this noise mechanism may be important in the design of a high-speed civil transport.[14] In an attempt to understand the nature of supersonic flows, much acoustic work has been performed for axisymmetric nozzle flows.[15–17]

The spatial structure of large-scale instabilities has been studied extensively using schlieren methods[18–21] as well as two-point acoustic measurements.[20,22] Unfortunately, the interpretation of azimuthally varying structures by the use of measurements in planes orthogonal to the nozzle exit plane is, of course, difficult.

Recent work[23] utilizing a circular microphone array in the exit plane of a round Mach 2 jet provided insight into the azimuthal variation of the near-field acoustic pressure associated with the preferred instability mode as manifest in the jet screech. The data presented in the current paper are the result of research on supersonic freejets emanating from an axisymmetric nozzle employing this technique. The technique has been substantially improved by application of new more efficient signal processing equipment and higher order spectral analysis methods. With the improved methods for signal acquisition and advances in high-order spectral processing (namely, the bispectrum), additional insight into the characteristics of preferred instability modes can be achieved.

Background

The dominant instability modes in supersonic freejet shear layers have been generally categorized in a simple manner: axisymmetric (or toroidal), spinning (single helix), and flapping (double helix). Past schlieren work[18,24] has indicated the B screech mode as being helical in nature (whether this mode is spinning or flapping is indeterminate by this optical technique alone). If one were to measure the instantaneous azimuthal pressure distribution about the jet axis created independently by the spinning and flapping modes, distributions as shown in Fig. 1 would be the result. Note that the distributions of Fig. 1 are computer generated models and are not actual measured results.

Figure 1a provides a pressure description of the spinning mode. This mode consists of an equal (azimuthally independent) amplitude pressure wave whose phase is azimuthally dependent. The instantaneous pressure distribution exhibits a spatial structure of period $2p$. This precessing of pressure about the jet axis is described as helical (single helix). Note that Fig. 1a could have also been plotted as a precession in the opposite direction. If two equal amplitude, oppositely rotating helical structures coexist, the result is the flapping mode (Fig. 1b). This figure shows the pressure as azimuthally dependent where mean square pressure maximums and minimums are orthogonal. Also notice that the phase is constant in 180-deg regions separated by the pressure minimums (nulls), and the phase shift between these regions is equivalent to one-half the period of the wave.

Figure 1 represents a qualitative means by which dominant shear layer instabilities are typically described. However, it should be remembered that these spatial descriptions are merely models which aid in understanding the large-scale instantaneous flow physics. This

Received Nov. 17, 1993; revision received Nov. 16, 1994; accepted for publication Nov. 28, 1994.

*Research Engineer, Aeroacoustics Branch. Member AIAA.
†Senior Research Engineer, Aeroacoustics Branch. Associate Fellow AIAA.

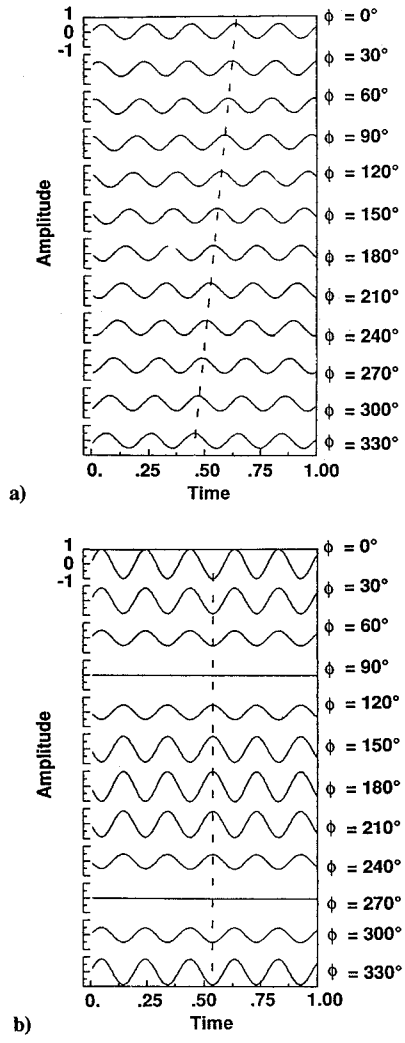

Fig. 1 Azimuthal pressure variations of different large scale structures: a) spinning structure and b) flapping structure.

set of models is not assumed to be complete (other modes may exist). Further, the fluctuating pressure is not, in reality, deterministic in space or time.

The frequency of jet screech and that for the most highly amplified instability wave are the same.[24] Thus, some understanding of the multimodal characteristics of large coherent structures may be gained by acoustic measurements. Ponton and Seiner[25] presented the wavelength of jet screech (normalized by the nozzle exit diameter) gathered from long duration spectral averages as a function of the fully expanded jet Mach number from near-field acoustic measurements of the round nozzle used for the current investigation. Screech is a multimodal phenomenon which undergoes discrete wavelength changes through a progression of operating pressures. This paper will focus on the B helical mode which has been shown[25] acoustically to be the dominant mode at $Mj = 1.3$. Ponton and Seiner[25] presented spectral changes in the B mode associated with lip thickness alterations; this paper will identify changes in the spatial characteristics for this mode.

Experimental Approach

The experiment was conducted in the Anechoic Noise Facility[26] at the NASA Langley Research Center. The interior dimensions of the facility within the wedge tips are 27.5 × 27 × 24 ft high. This anechoic treatment absorbs at least 99% of incident sound at frequencies greater than 100 Hz. The air system is capable of supplying continuous dry unheated air at mass flow rates of 10 lb/s and at maximum stagnation pressures of 255 psig (muffler system limit). Electronically controlled valves maintain nozzle pressure ratios to within 0.3% of the set point. All pressure transducers used in the flow control system received daily calibration.

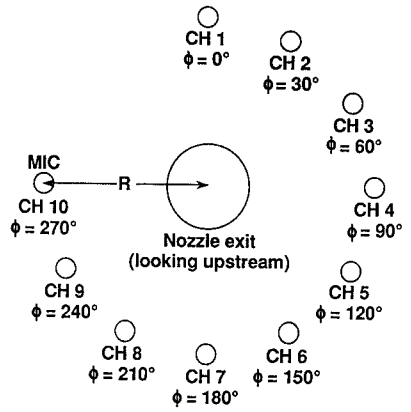

Fig. 2 Microphone positions about the nozzle periphery.

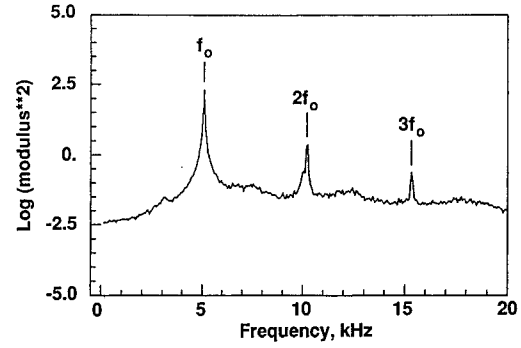

Fig. 3 Spectrum showing the dominant B mode at frequency f_0, CH 1, $R/D = 2$.

The axisymmetric nozzle assembly consisted of a contoured transition section connecting a 7.875 in. i.d. supply air pipe to a 1.500-in. i.d. pipe, which then led to the nozzle. The 1.500-in. straight section was 26.01 in. long with an outside diameter of 2.250 in. The length of this assembly was selected to minimize acoustic reflections from the flange and interference to the jet entrainment. The nozzle was convergent and conical (5-deg convergence angle) with an exhaust diameter of 1.000 in. and an exit lip thickness of 0.015 in. A high-precision collar was fabricated which, when placed over the nozzle exit, would increase the nozzle exit lip thickness to 0.625 in. This external geometry alteration has been shown[25] to affect the plume's preferred mode of instability.

In the nozzle exit plane, spaced at 30-deg intervals, 10 1/4-in.-diam. microphones were placed (Fig. 2). No protective grid cap was used during data recording. Phase matching through the system (excluding transducer diaphragms) was checked using white noise input up to 40 kHz. The data were bandpass filtered from 100 Hz to 20 kHz and then digitized using 10 channels of 12-bit analog-to-digital converters sampling at 125 kHz; 131072 data points per channel were stored.

Experimental Results

0.015-in. Exit Lip Thickness

At $Mj = 1.30$, the preferred instability mode is the B mode, as indicated by the dominant narrow-band process at 5.127 kHz for the microphone 1 spectrum at $R/D = 2$ (Fig. 3). Figure 4 contains the time trace for the first millisecond of acoustic pressure data. (The amplitude is the microphone output, in volts, normalized by the output voltage for a fixed calibration pressure input; thus, normalized voltage is linearly related to acoustic pressure.) The similarity between this figure and Fig. 1b indicates the presence of a jet flapping mode. Note the low-amplitude waves at opposite positions of the jet ($f = 60$ and 240 deg) and the phase shift in regions separated by these near nulls equal to one-half the period of the screech frequency (see plotted vertical lines). The shape of these pressure waves deviates from a pure sinusoidal wave due to the presence of strong harmonics (Fig. 3). The flapping plane is

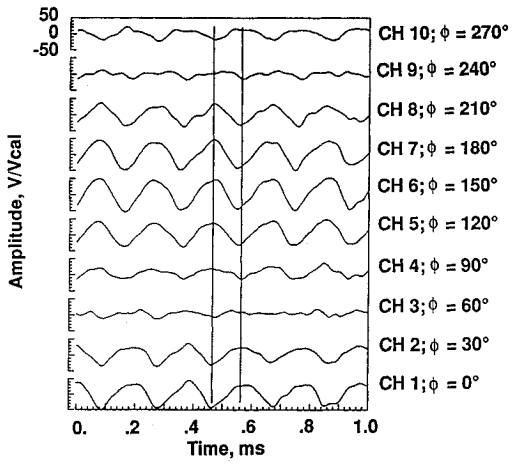

Fig. 4 Time trace of 1 ms at $R/D = 2$.

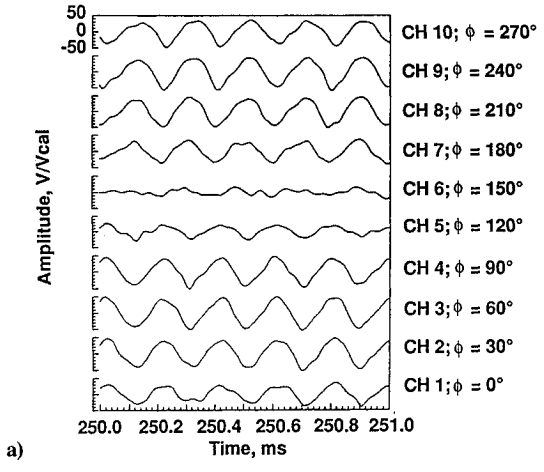

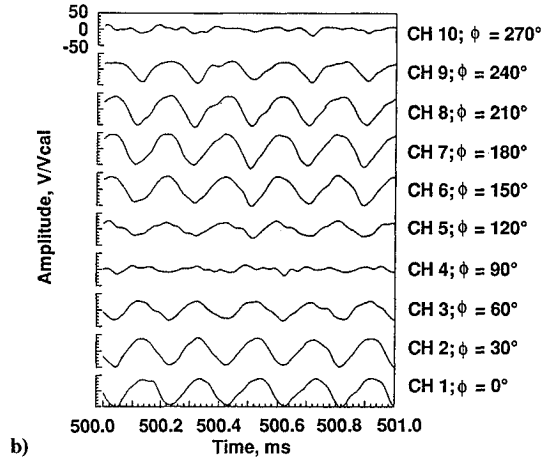

Fig. 5 Time traces for different 1-ms time intervals: a) $T_0 = 0.25$ s and b) $T_0 = 0.50$ s.

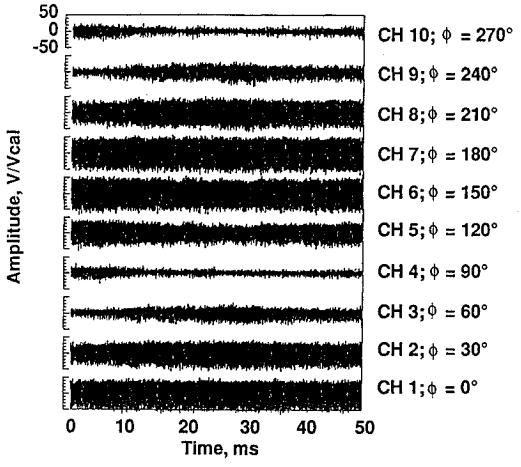

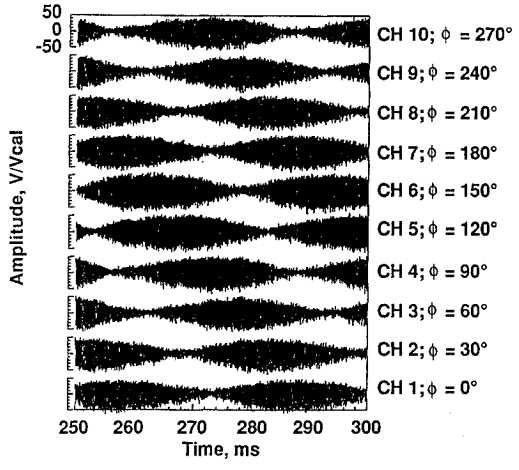

Fig. 6 Time traces for different 50-ms time intervals: a) $T_0 = 0.00$ s and b) $T_0 = 0.25$ s.

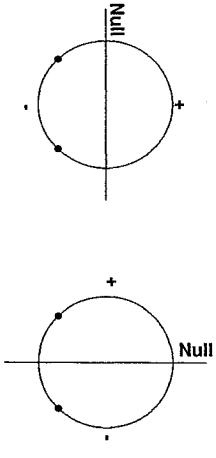

Fig. 7 Phase change due to a rotation of the flapping structure.

defined as the plane which encompasses the dominant motion of the jet; thus, for Fig. 4 the flapping plane can be defined using the jet axis and microphone 6.

Figures 5a and 5b are 1-ms time records 1/4 and 1/2 s later than those of Fig. 4, respectively. The (near) null position in Fig. 5a is now $f = 150$ deg whereas in Fig. 5b it is 90 and 270 deg. This indicates that the orientation of the flapping plane is a function of time.

To better observe this variability, longer time records are presented (Figs. 6a and 6b). The first 50 ms of the time record (Fig. 6a) indicates no large changes in flapping direction, but 250 ms later (Fig. 6b) large changes are observed. This periodic motion seen in Figure 6b is hypothesized as being a rotation of the flapping structure about the jet axis.

Establishing the existence of such a rotation involved the following reasoning. If two sensors (closed circles on Fig. 7) are located on the same side of the null line (this line is perpendicular to the flapping plane), then their respective fluctuating pressures are in phase (left side of Fig. 7). If now the flapping plane rotates, the pressure null at some time can then be positioned between the sensors, and thus their respective pressure will be out of phase (right side of Fig. 7). This reasoning was applied to the data for the time interval from 282 to 294 ms where it is observed in Fig. 6b that the microphone 4 data contain an amplitude minimum at approximately 288 ms and the microphone 1 data contain no significant amplitude

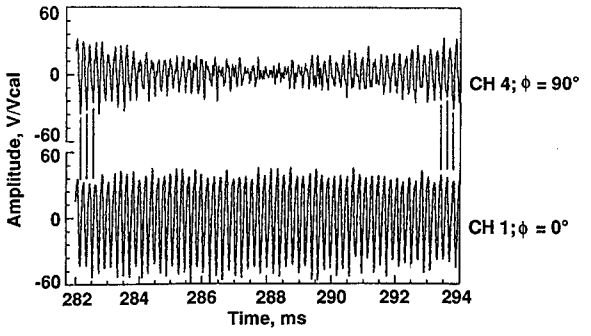

Fig. 8 Identified phase change for microphone measurements indicating a rotating flapping structure.

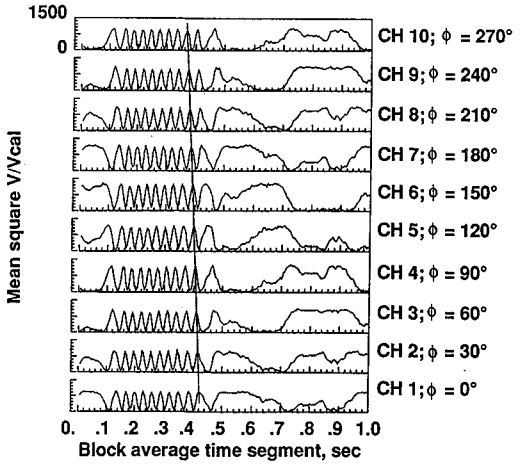

Fig. 9 Mean square pressure variation at $R/D = 2$.

deviations and thus should be of constant phase within this interval. Figure 8 is a plot of this time interval. As is shown by the vertical lines, prior to the microphone 4 pressure minimum, the two signals are in phase; following the minimum, they are out of phase. If this reasoning is correct, this is an indication of a rotation of the flapping structure.

The method employed to describe the amplitude variation with azimuthal position as well as with time is to plot the mean square amplitude where averaging was performed over 5-ms blocks over a total time interval of 1 s. Thus the mean square amplitude from 0 to 0.005 s is plotted at 0.005 s (on the abscissa), the mean square amplitude from 0.005 to 0.010 s is plotted at 0.010 s, and so on.

The mean square amplitude variation is presented in Fig. 9. Because the azimuthal pressure maximums and minimums have distinct orientations (i.e., orthogonal), this plot should lend insight into the nature of this rotating behavior. As is shown in this figure, the time interval of rapid rotation occurs between 0.1 and 0.4 s. Note that these block averages are over 5 ms, which should be sufficiently small when compared to the period of this rapid rotating action as shown in Fig. 6b. This rotating action appears random over the interval plotted in Fig. 9.

The slope of a line of constant phase will be an indicator of the direction of this rotating motion. The line plotted on Fig. 9 would indicate the rotating motion to be counterclockwise when viewing upstream toward the nozzle exit (see Fig. 2). The data collected at $R/D = 4$ (Fig. 10) indicate that this rotation direction is not unique. ($R/D = 4$ data were used to note the nonuniqueness of the rotation direction because the time record for the $R/D = 2$ data did not contain a direction reversal; however, it is anticipated that such a direction reversal would be identified for a measurement location of $R/D = 2$ if additional data would have been collected.) Note the change of direction from counterclockwise to clockwise at approximately the 0.25 s block in Fig. 10. Also notice that the rotation frequency appears to increase from 0.25 to 0.72 s and then to decrease after 0.72 s, as indicated by the time interval between mean square pressure maximums. Although the B mode is essentially a

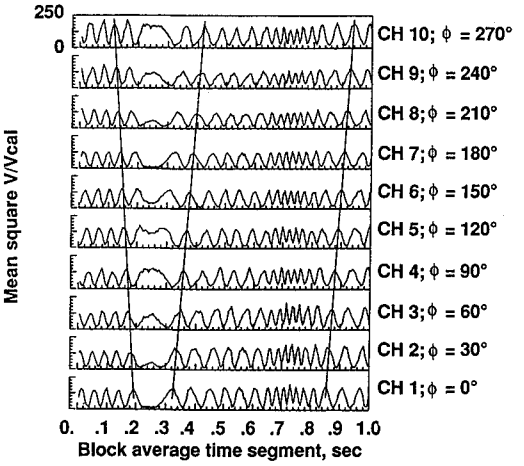

Fig. 10 Mean square pressure variation at $R/D = 4$.

flapping mode, a seemingly random rotation of the flapping orientation is observed to exist. The time period of this random rotation is seen to be as much as two orders of magnitude greater than the screech period.

0.625-in. Exit Lip Thickness

Presented in Fig. 11 are various 1-ms time records for the 0.625-lip thickness nozzle operating at $Mj = 1.30$ where the dominant instability mode is the B mode. Initially (Figs. 11a and 11b), the pressure distribution is indicative of a flapping structure as previously characterized. But now notice that after a short time interval (Figs. 11c and 11d) the pressure amplitude is better represented by a spinning wave (see Fig. 1a). Figure 11e indicates a return of the flapping structure and Figs. 11e–11g show a flapping-spinning-flapping transition of structures over a 1/4-s interval. This behavior was not observed for the thin-lipped configuration. Thus, at this Mach number, the increase in exit lip thickness has altered the characteristics of the plume's preferred instability mode. Figure 12 presents the mean square amplitude variation for this operating condition. From this plot, time periods of rapid mean square oscillations for all microphone channels are seen in the intervals of (approximately) 0–0.12 s, 0.65–0.78 s, and 0.98–1.00 s. Interestingly, during these intervals, the azimuthal pressure distribution is more characteristic of a flapping structure (Figs. 11a, 11b, 11e, and 11g), whereas less oscillatory mean square intervals are seen to behave more like spinning modes (Figs. 11c, 11d, and 11f). Because analysis of the entire time interval recorded is difficult (due to its magnitude), it would be premature to assume that an oscillatory mean square distribution (for this operating condition and nozzle configuration) is a concomitant to a flapping mode.

If a 150-ms time interval is plotted (Fig. 13), one can identify regions where phase reversal (indicative of a slowly rotating flapping structure) may occur. Such a region is plotted in Fig. 14 where a phase change is observed to occur through microphone 4's pressure minimum (at approximately 87 ms) when compared to an unvarying phase reference (microphone 1), as noted by the vertical lines. This suggests that when the large-scale structure is flapping, a rotation about the jet axis also occurs, as was seen for the thin-lipped configuration.

Using wave modeling analysis, a distinction can be made between a rotating flapping structure and a time-dependent flapping/spinning structure. Recall that a flapping mode is modeled as the summation of two equal amplitude but oppositely rotating helices. If the amplitude of one of the helical structures varies with time, then the azimuthal pressure distribution would also change its characteristics from flapping to spinning (or vice-versa) in the limiting cases, i.e., those cases where both amplitudes are equal (flapping) or when one amplitude is zero (spinning). Nonlimiting cases would give a pressure distribution whose characteristics would not be a perfect spinning or flapping motion. However, this amplitude mismatch (i.e., different nonzero amplitude oppositely rotating helices) would not cause a variance in the azimuthal angle at which the mean square

pressure wave is a minimum. As is evident in Figs. 5 and 11, the azimuthal angle of minimum pressure amplitude varies with time. A possible cause of such an effect would be an alteration in the phase difference between the two oppositely rotating helices. Thus, in summary, a time dependent flapping/spinning structure (thick-lipped B mode) can be caused by variance in time of the amplitudes of two oppositely rotating helical structures; a time dependence in the azimuthal orientation of pressure minimums (i.e., the rotating flapping structure seen for both lip thicknesses tested) may be attributed to a variance in time of the phase difference between the two helical structures. The distinction should be noted that a rotation of the large-scale flapping structure and a spinning structure are presumed to be different phenomena.

Bispectral Analysis

Figure 15 is a spectral comparison between the thick- and thin-lipped nozzle configurations (64 averages, record length 16.384 ms). As is evident, the frequency of the dominant mode has decreased from (approximately) 5.1 kHz to 5 kHz when the exit lip thickness is increased. This behavior was observed by previous research[25] and could be the result of a change in the plume's most amplified (preferred) instability wave and/or the convection velocity. There is also an increase in amplitude between 7 and 7.5 kHz for the thick-lipped nozzle spectrum. Recall that the time-dependent flapping/spinning behavior for the thick-lipped nozzle was explained by time-dependent amplitude changes in two oppositely rotating helical structures. Thus, the additional spectral components seen for the thick-lipped model may indicate a nonlinear interaction between the dominant large-scale structure (B mode) and additional shear layer structures which could explain the aforementioned amplitude modulations. To determine if nonlinearities are present in the acoustic measurements, a bispectral analysis was performed on the data.

If we model the measured fluctuating pressure time record at a point in space with the Fourier representation

$$p(t) = \int_{-\infty}^{\infty} P(f) e^{i2\pi ft}\, df$$

where $P(f_m)$ is the complex Fourier amplitude at frequency f_m; then the wave coupling of frequencies f_k and f_l with f_m, where $f_m = f_k + f_l$ (note that in the second harmonic case $f_k = f_l$), can be identified using the autobicoherence spectrum[27]

$$b^2(f_k, f_l) = \frac{|B(f_k, f_l)|^2}{E\left[|P_k P_l|^2\right] \cdot E\left[|P_m|^2\right]}$$

where $E[\,]$ is the expectation operation, and $B(f_k, f_l)$ is the autobispectrum defined as

$$B(f_k, f_l) = E[P_k P_l P_m^*], \qquad m = k + l$$

Note that the bispectrum was developed for nonlinear, stationary random processes. As indicated by the time dependence of the mean square pressure, the measured data indicate a nonstationary process. Thus, the use of the bispectral analysis requires some justification.

If $X(t)$ is a mean zero process (such as the measured acoustic signals), i.e.,

$$E[X(t)] = 0 \tag{1}$$

then the expected value of the Fourier transform of the signal $X(t)$ can be given by

$$E[X(f)] = \frac{1}{2\pi} \int_{-\infty}^{\infty} E[X(t)] e^{i2\pi ft}\, dt = 0 \tag{2}$$

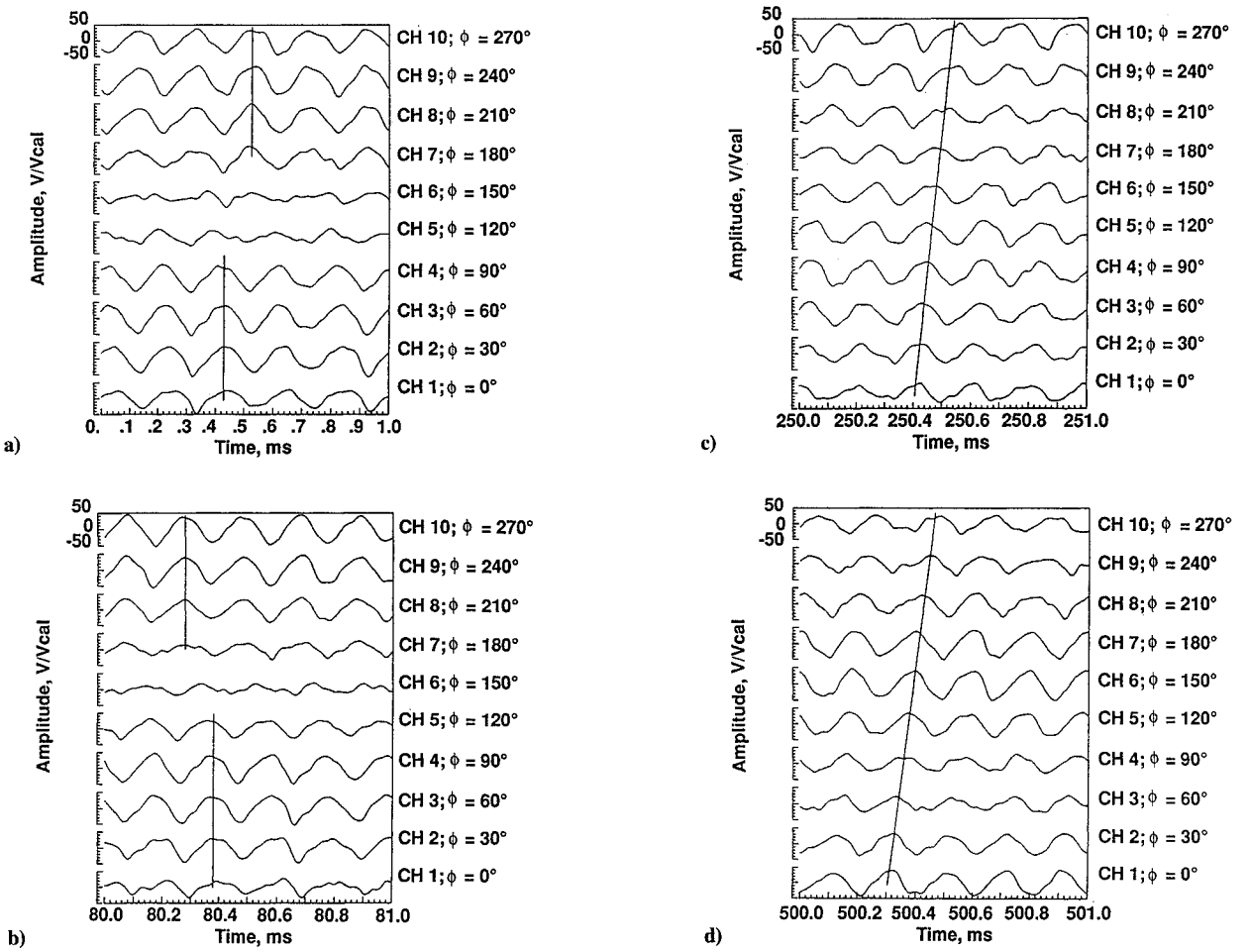

Fig. 11 Time traces of 1 ms for the 0.625-in. lip thickness: a) T_0 = 0.00 s, b) T_0 = 0.08 s, c) T_0 = 0.25 s, d) T_0 = 0.50 s, e) T_0 = 0.75 s, f) T_0 = 0.90 s, and g) T_0 = 1.00 s.

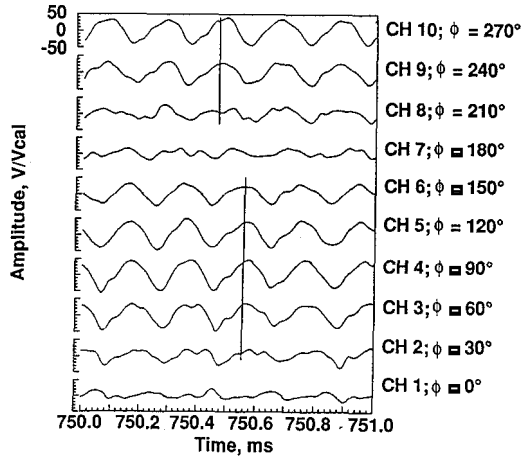

e)

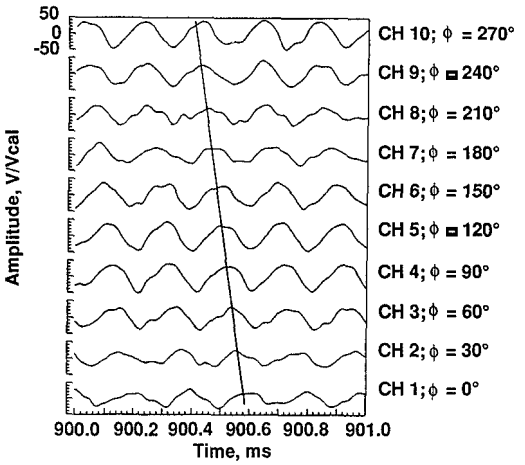

f)

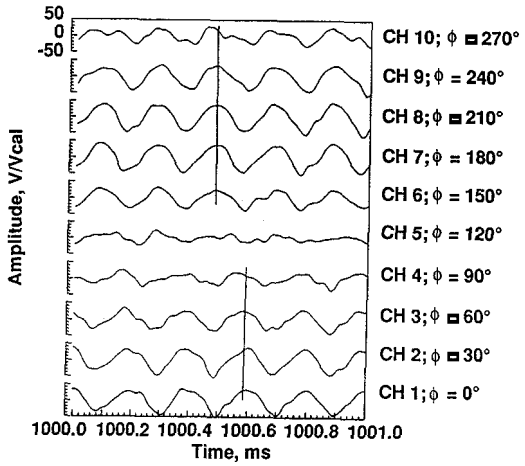

g)

Fig. 11 (Continued) Time traces of 1 ms for the 0.625-in. lip thickness: a) T_0 = 0.00 s, b) T_0 = 0.08 s, c) T_0 = 0.25 s, d) T_0 = 0.50 s, e) T_0 = 0.75 s, f) T_0 = 0.90 s, and g) T_0 = 1.00 s.

from relation (1). Now consider the triple spectral correlation

$$E[X(f_1)X(f_2)X^*(f_3)]$$

for a nonstationary, mean zero process. If $X(f_1)$, $X(f_2)$, and $X(f_3)$ are independent (and therefore uncorrelated), then

$$E[X(f_1)X(f_2)X^*(f_3)] = E[X(f_1)]E[X(f_2)]E[X^*(f_3)] = 0$$

from relation (2). If $X(f_1)$, $X(f_2)$, and $X(f_3)$ are dependent, then

$$E[X(f_1)X(f_2)X^*(f_3)] \neq 0$$

in general.[28] Thus, the computation of the bispectrum in this paper is not an assumption of stationarity but rather is used as an indicator

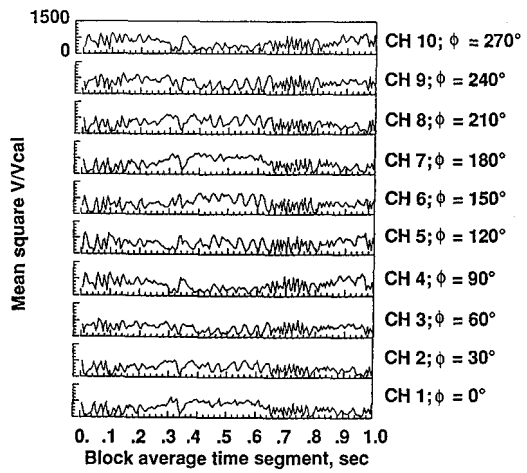

Fig. 12 Mean square pressure variation, 0.625-in. lip, R/D = 2.

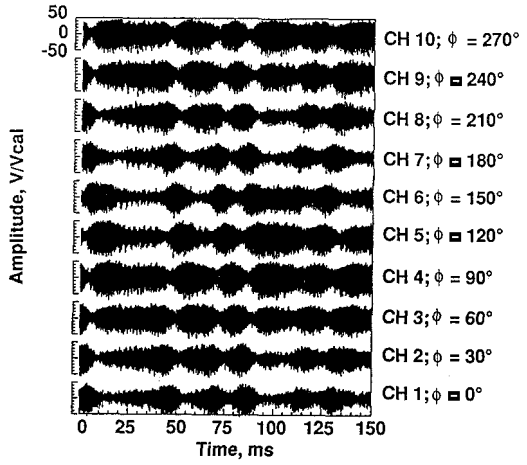

Fig. 13 Time trace of 150 ms, 0.625-in. lip, R/D = 2.

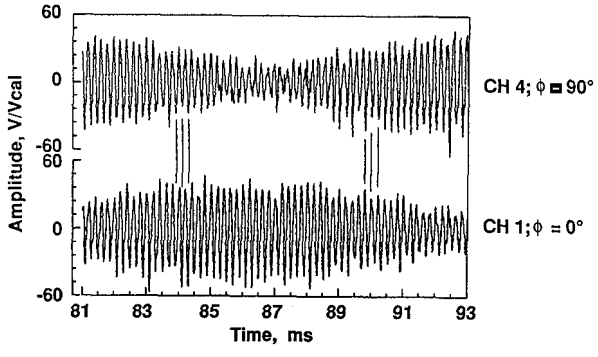

Fig. 14 Phase shift indicative of a rotating flapping structure, 0.625-in. lip.

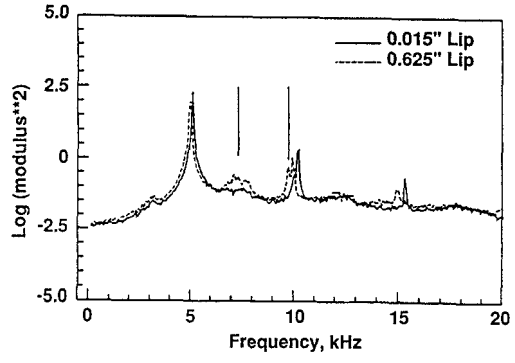

Fig. 15 Spectral comparison between the 0.015-in. and 0.625-in. lip thickness, CH 1.

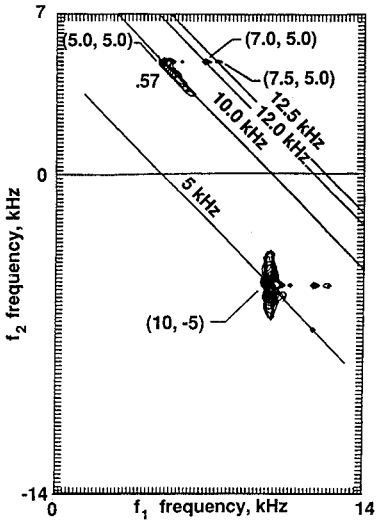

Fig. 16 Squared autobicoherence spectrum for the microphone 1 measurement, R/D = 2, of the 0.625-in. lip thickness.

of the dependence of three spectral components whose frequencies satisfy the selection criteria $f_3 = f_1 + f_2$.

Nonlinear wave-wave interactions result in the formation of new spectral components which are phase coherent (a phase relationship between independently excited modes would not be expected). These nonlinear interactions encompass not only quadratic interactions ($f_m = f_k + f_l$, $f_k \neq f_l$) and harmonic generation ($f_m = 2 \times f_k$) but also more complex interactions of unknown nature. In the limiting case where only three power spectral components f_1, f_2, and f_3 are present and the only nonlinear interaction is quadratic (creating $f_3 = f_1 + f_2$), the autobicoherence would be an indicator of the fraction of power of the f_3 wave due to the coupling of the f_1 and f_2 waves. However, because of the possibility of more complex nonlinear interactions (for example, $f_4 = f_1 + f_2 + f_3$), the autobicoherence, in general, is not a fractional power measure but an indicator of phase coherence between nonlinearly coupled waves.[27]

Figure 16 presents the squared autobicoherence spectrum of the microphone 1 data for the thick-lipped nozzle operating at $Mj = 1.30$. The minimum value plotted is 0.1 (minimum autobicoherence level of 32%) and the spectral resolution is 178.6 Hz where 128 averages were performed (record length 5.6 ms). The diagonal lines are lines of constant $f_3 = f_1 + f_2$ which corresponds to the selection criteria of the bispectrum. Locations of high autobicoherence indicated by the dark regions signify three frequencies (f_1, f_2, f_3) which have a nonlinear relationship as manifest by their phase coupling. For example, the upper diagonal line represents $f_3 = 12.5$ kHz. The dark region on this line has an f_1 value of 7.5 kHz and an f_2 value of 5.0 kHz. This indicates a nonlinear relationship between the 5.0, 7.5, and 12.5 frequency components. Also evident on this figure is a nonlinear interaction between the 5.0, 7.0, and 12.0 frequencies. Although not presented, a similar bispectral analysis for the thin-lipped configuration did not reveal the presence of similar nonlinearities as seen for the thick-lipped nozzle. These additional nonlinear interactions for the 0.625-in. exit lip thickness may indicate an energy transference between various flow structures which could be related to an amplitude modulation of the two oppositely rotating helical structures. As previously discussed, this could cause the observed time-dependent flapping/spinning characteristics for this nozzle configuration.

Concluding Remarks

The objective of this research was to gain further insight into the spatial characteristics of dominant large-scale structures associated with supersonic axisymmetric flows. In particular, this paper has presented data on the B helical instability mode for an underexpanded conical nozzle utilizing two exit lip thicknesses.

The data indicate that for the thin-lipped nozzle, the B mode is a flapping mode which precesses about the jet axis in a seemingly random fashion. For a flapping structure modeled as two equal amplitude, oppositely rotating helical structures, this behavior may be a time dependence in the relative phasing between the two helices.

For the thick-lipped configuration, the B mode becomes a time-dependent flapping/spinning structure. This structure may be due to a time dependence of the amplitudes corresponding to the two oppositely rotating helices. A bispectral analysis revealed additional nonlinear interactions associated with the thick-lipped geometry which may account for the proposed amplitude modulations. New models that account for the observed nonlinearities are needed to accurately predict the acoustic field generated by the large-scale structures.

It should be remembered that the aerodynamic conclusions made are based on acoustic measurements and not on in-flow dynamic measurements. These latter measurements, although difficult to perform, should be a future goal to determine if the observed nonlinearities are fluid structure interactions or are the result of nonlinear propagation effects through the ambient medium.

Acknowledgments

The authors would like to thank Jay C. Hardin for his assistance in justifying the use of the bispectral analysis for a nonstationary random process. This work contains the results of research performed for a thesis submitted to the George Washington University in partial fulfillment of the requirements for the Master of Science degree.

References

[1]Hinze, J. O., *Turbulence*, McGraw-Hill, New York, 1959, pp. 1–72.

[2]Tennekes, H., and Lumley, J. L., *A First Course in Turbulence*, MIT Press, Cambridge, MA, 1972, pp. 27–58.

[3]Michalke, A., "On Spatially Growing Disturbances in an Inviscid Shear Layer," *Journal of Fluid Mechanics*, Vol. 23, Pt. 3, Nov. 1965, pp. 521–544.

[4]Brown, G. L., and Roshko, A., "Density Effects and Large Structure in Turbulent Mixing Layers," *Journal of Fluid Mechanics*, Vol. 64, Pt. 4, July 1974, pp. 775–816.

[5]Cohen, J., and Wygnanski, I., "The Evolution of Instabilities in the Axisymmetric Jet," *Journal of Fluid Mechanics*, Vol. 176, March 1987, pp. 191–219.

[6]Tam, C. K. W., and Morris, P. J., "The Radiation of Sound by the Instability Waves of a Compressible Plane Turbulent Shear Layer," *Journal of Fluid Mechanics*, Vol. 98, May 1980, pp. 349–381.

[7]Gaster, M., Kit, E., and Wygnanski, I., "Large-Scale Structures in a Forced Turbulent Mixing Layer," *Journal of Fluid Mechanics*, Vol. 150, Jan. 1985, pp. 23–39.

[8]Ho, C. M., and Huerre, P., "Perturbed Free Shear Layers," *Annual Review of Fluid Mechanics*, Vol. 16, 1984, pp. 365–424.

[9]Seiner, J. M., Mclaughin, D. K., and Liu, C. H., "Supersonic Jet Noise Generated by Large-Scale Instabilities," NASA TP-2072, Sept. 1982.

[10]Tam, C. K. W., Seiner, J. M., and Yu, J. C., "Proposed Relationship Between Broadband Shock Associated Noise and Screech Tones," *Journal of Sound and Vibration*, Vol. 110, No. 2, 1986, pp. 309–321.

[11]Powell, A., "Mechanism of Choked Jet Noise," *Proceedings of the Physical Society, London*, Vol. 66, Pt. 12, Dec. 1953, pp. 1039–1056.

[12]Seiner, J. M., Manning, J. C., and Ponton, M. K., "Model and Full Scale Study of Twin Supersonic Plume Resonance," AIAA Paper 87-0244, Jan. 1987.

[13]Hay, J. A., and Rose, E. G., "In-flight Shock Cell Noise," *Journal of Sound and Vibration*, Vol. 11, No. 4, 1970, pp. 411–420.

[14]Seiner, J. M., and Krejsa, E. A., "Supersonic Jet Noise and the High Speed Civil Transport," AIAA Paper 89-2358, July 1989.

[15]Seiner, J. M., and Norum, T. D., "Experiments of Shock Associated Noise on Supersonic Jets," AIAA Paper 79-1526, July 1979.

[16]Norum, T. D., and Seiner, J. M., "Measurements of Mean Static Pressure and Far-Field Acoustics of Shock-Containing Supersonic Jets," NASA TM-84521, Sept. 1982.

[17]Seiner, J. M., and Ponton, M. K., "Aeroacoustic Data for High Reynolds Number Supersonic Axisymmetric Jets," NASA TM-86296, Jan. 1985.

[18]Davies, M. G., and Oldfield, D. E. S., "Tones from a Choked Axisymmetric Jet," *Acoustica*, Vol. 12, No. 4, 1962, pp. 257–277.

[19]Poldervaart, L. J., Vink, A. T., and Wijands, A. P. J., "The Photographic Evidence of the Feedback Loop of a Two Dimensional Screeching Supersonic Jet of Air," *The 6th International Congress on Acoustics*, F-3-9, 1968, pp. 101–104.

[20]Westley, R., and Woolley, J. H., "The Near Field Sound Pressures of a Choked Jet During a Screech Cycle," *AGARD Conference Proceedings*, AGARD, Neuilly-sur-Seine, France, 1969, pp. 23-1–23-13 (No. 42).

[21]Matsuda, T., Umeda, Y., Ishii, R., and Yasuda, A., "Numerical and Experimental Studies on Choked Underexpanded Jets," AIAA Paper 87-1378, June 1987.
[22]Westley, R., and Woolley, J. H., "The Near Field Sound Pressures of a Choked Jet When Oscillating in the Spinning Mode," AIAA Paper 75-479, March 1975.
[23]Seiner, J. M., Manning, J. C., and Ponton, M. K., "The Preferred Spatial Mode of Instability for a Mach 2 Jet," AIAA Paper 86-1942, July 1986.
[24]Seiner, J. M., "Advances in High Speed Jet Aeroacoustics," AIAA Paper 84-2275, Oct. 1984.
[25]Ponton, M. K., and Seiner, J. M., "The Effects of Initial Jet Exit Conditions on Plume Resonance," AIAA Paper 89-1054, April 1989.
[26]Hubbard, H. H., and Manning, J. C., "Aeroacoustic Research Facilities at NASA Langley Research Center—Description and Operational Characteristics," NASA TM- 84585, March 1983.
[27]Miksad, R. W., Jones, F. L., and Powers, E. J., "Measurements of Nonlinear Interactions During Natural Transition of a Symmetric Wake," *Physics of Fluids*, Vol. 26, No. 6, 1983, pp. 1402–1409.
[28]Hardin, J. C., Private communication, NASA Langley Research Center Hampton, VA, Jan. 1991.